Friction Stir Welding – an Advanced Approach to Repair Nuclear Power Plant Components

W. Tang
Materials Science and Technology Division
Oak Ridge National Laboratory
1 Bethel Valley Road
Oak Ridge, TN 37831-6079
USA

X. Chen
Materials Science and Technology Division
Oak Ridge National Laboratory
1 Bethel Valley Road
Oak Ridge, TN 37831-6136
USA

M. Gussev
Nuclear Energy and Fuel Cycle Division
Oak Ridge National Laboratory
1 Bethel Valley Road
Oak Ridge, TN 37831-6136
USA

T. M Rosseel
Materials Science and Technology Division
Oak Ridge National Laboratory
1 Bethel Valley Road
Oak Ridge, TN 37831-6132
USA

ABSTRACT

Solid phase joining technique friction stir welding (FSW) has been shown to mitigate helium-related issues in fusion welding of irradiated steels. Here, we present detailed characterization results of the first friction stir weld of an irradiated 304L stainless steel (SS) coupon contained 5.2 atomic parts per million (appm) helium. Scanning electron microscopy (SEM) was used to characterize a cross-section specimen extracted from the friction stir weld. No macro helium induced crack was observed at the analyzed cross-section, and only 1 – 1.5 μm size pores were found in the stir zone (SZ) and the thermal-mechanical affected zone (TMAZ). Moreover, some minor helium aggregations (Maximum ~20 μm in length) appeared along grain boundaries inside the TMAZ. Thereafter, miniature tensile specimens were extracted from the SZ, TMAZ and heat affected zone (HAZ), and base metal (BM) and tested. All welded specimens showed high total elongations (> 60%) and strengths (> 75% BM strengths). Overall, the weld made by FSW showed much better results comparing with traditional fusion welding on irradiated SS.

Key words: Friction stir welding, Irradiated stainless steel, Microstructure, Mechanical properties.

INTRODUCTION

The harsh environment such as high temperature, radiation, elevated pressure, and potentially corrosive in nuclear reactors compromises material performance. Over time, Repair and/or replacement through welding is needed for damaged parts and components. Thus, repair welding is essential to ensure the long-term viability, competitiveness, and safe lifetime extensions of the existing US reactor fleet.

Fusion welding techniques such as gas tungsten arc welding (GTAW) and gas metal arc welding (GMAW) are widely used in nuclear power plant (NPP) construction to assemble structural material components. However, fusion welding repair of NPP irradiated components meets one specific issue: helium-induced cracking [1 – 3]. Neutron fluxes stimulate transmutation reactions in the NPP core materials and lead to helium formation from boron impurity and nickel element.

$$^{10}B + n \rightarrow {}^{7}Li + {}^{4}He \quad (1)$$
$$^{58}Ni + n \rightarrow {}^{59}Ni + \gamma \quad (2)$$
$$^{59}Ni + n \rightarrow {}^{56}Fe + {}^{4}He \quad (3)$$

Helium transmutation and accumulation are especially severe in water-moderated reactors because of the “soft” neutron spectra with a high fraction of thermal neutrons. Helium distributes in metals as individual atoms due to its insoluble in steels. With the high heat input in fusion welding, helium migrates at grain boundaries (GBs) and forms bubbles, which drastically reduces the GB strength. At the same time, the local transient elevated temperatures during fusion welding result in high tensile stresses in the weld zone (WZ) and heat affected zone (HAZ). The combination of degraded GB strengths and the high tensile stress can easily initiate crack formation on the helium-compromised GBs and lead to the crack propagation, i.e., helium induced cracking.

Applying welding on steels containing 1–3 atomic parts per million (appm) of helium may induce helium cracking in welding, and steels with more than 10 appm of helium are often considered nonweldable with today’s fusion welding techniques [1 – 6]. In general, critical helium concentrations (above 1–3 appm) may be reached even for peripheral parts within ~10 – 20 years, which time is much lower than the planned life span of typical NPPs (40 years), not to mention the extension (to ~60 – 80+ years) of NPPs. Therefore, helium-induced cracking is the major barrier of applying fusion welding to repair structural materials in NPP after years of service.

In 1986, the GTAW technique was used to repair the water leakage of a Savannah River National Laboratory reactor, and many cracks were presented at the HAZ after repair welding attempts. The cracks resulted in the reactor’s permanent shutdown. Investigation showed that these were helium-induced cracks, and helium concentration in the repaired water tank wall was ~3 appm [1]. In a study applying GTAW on irradiated stainless steel containing 8.3 appm of helium, many several millimeters long cracks were observed in the HAZ [2]. Studies have shown that elevated temperatures and the appearance of tensile stress in cooling of a fusion welding are two key factors in helium-induced crack formation and propagation [7].

Friction Stir Welding (FSW) is an advanced manufacturing technology [8, 9] with peak temperatures much lower than the material bulk melting point (generally between 0.6–0.8 T_m). During FSW, the material is heated up by friction between the welding tool and welded material, as well as by plastic deformation of the material being welded. Heated material flows/deforms around the welding tool and forms a joint, as the result of mechanical mixing and recrystallization [10]; tool wear during high temperature materials, such as steel and stainless steel, FSW is often mentioned [11].

FSW is arguably the most recent significant invention in welding technologies, and it has been widely studied and developed. In many applications, FSW demonstrated outstanding weldability to form high-quality joints with excellent mechanical properties. Lower peak temperatures and shorter time at elevated temperature, compared to traditional fusion welding techniques, can significantly reduce the intensity of diffusion-based processes, including helium migration. The low peak temperatures may also reduce tensile thermal stresses. These considerations make the FSW a potential solution for irradiated structural materials containing helium repairing.

Although being promising, the FSW had not been used for joining irradiated materials containing significant amount of helium until Oak Ridge National Laboratory's (ORNL's) team successfully demonstrated FSW on irradiated 304L stainless steel (304L SS) for the first time at the end of 2017 [10, 12, 13].

In this paper, advanced characterization techniques were used to characterize the helium-containing friction stir weld, with a particular focus on grain microstructure and mechanical properties.

EXPERIMENTAL PROCEDURE

Material and Condition

The material used in the study is an irradiated 304L stainless steel (SS) friction stir weld, which was joined at ORNL by the end of 2017 [10, 12, 13]. Prior to the FSW, boron was added in the material through arc melting followed by extrusion, and helium was formed in the boron dopped coupon through neutron irradiation. The helium was detected 5.2±1.1 appm in the irradiated 304L SS coupon using thermal desorption spectrometry. The friction stir weld specimen dimensions were 1.2 × 0.35 × 0.1 in.

Microstructure Characterization

A TESCAN MIRA3 Scanning electron microscopy (SEM) was used to conduct general microstructure analysis and electron backscatter diffraction (EBSD) was used for grain structures. The SEM is equipped with an advanced Oxford Symmetry EBSD detector (resolution 1244×1024 pixels, indexing rate up to ~200 Hz in full-frame mode, and ~3.5 kHz in 8×8 binning mode). All EBSD scans were performed at 20 kV; step size varied from 0.125 to 1 micron, depending on the region and feature of interest. The friction stir weld specimen surface was surveyed using both SE (secondary electron image) and BSE (backscatter electron image) detectors.

Mechanical property examination

After microstructure characterization, miniature tensile specimens, were machined from the irradiated 304L SS friction stir weld cross-section specimen. There are three tensile specimen conditions which gauge areas contained stir zone (SZ) only, thermal mechanical affected zone (TMAZ) and HAZ, and base metal (BM) only, respectively. The tensile specimen IDs and locations are shown in Table 1. The miniature tensile specimen design and assembled on the tensile frame setup are shown in Figure 1.

Table 1 Room temperature tensile test specimen ID, location, and condition

Specimen ID	Locations	Conditions
304C-6-14-2	Weld ¼ depth advancing side	Gauge contains TMAZ and HAZ
304C-6-14-4	Weld ¼ depth retreating side	Gauge contains TMAZ and HAZ
304C-6-14-6	Weld root	Gauge contains TMAZ and HAZ
304C-6-14-8	Weld ¼ depth SZ middle	Gauge contains SZ
304C-6-14-16	BM	Gauge contains BM

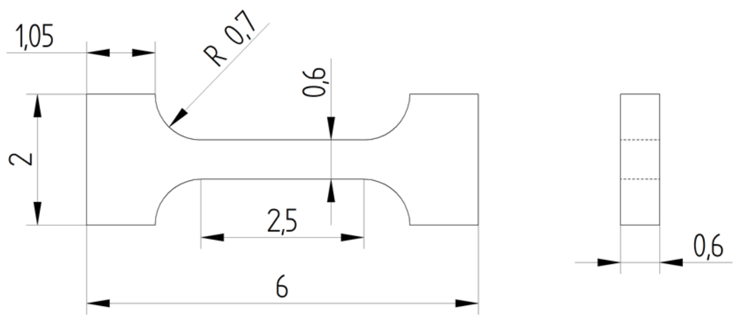

(a) Miniature tensile specimen design. Unit: mm

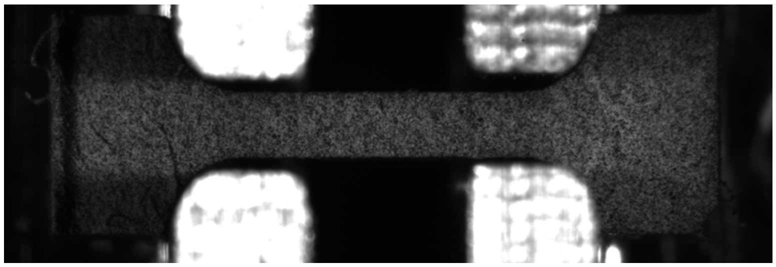

(b) A DIC miniature tensile specimen with speckle pattern.

Figure 1. DIC miniature tensile specimen

The pulling rate of the tensile tests was 0.025 mm/s. The strain and elongation were measured from an initial 2.5 mm gauge length using digital image correlation (DIC) technique.

RESULTS

Microstructure Characterization

The cross-section specimen of the irradiated 304L friction stir weld is shown in Figure 2. Without etching, different metallurgical zones are not clearly seen. Therefore, dotted lines were added in Figure 2 to demonstrate SZ, TMAZ and BM schematically. It is clear that this cross section doesn't contain any macro level voids or helium induced crack which usually seen in WZ and HAZ of irradiated steel fusion welds [1 – 6].

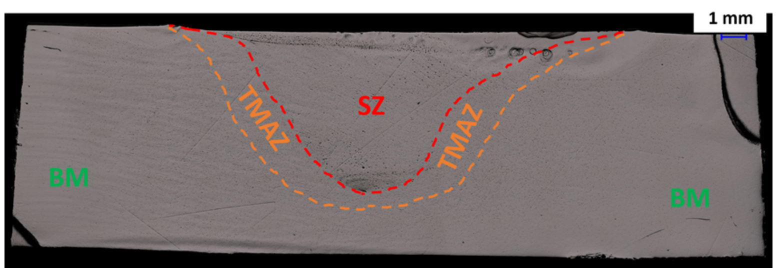

Figure 2. Irradiated 304L SS friction stir weld cross section.

In the SZ, ~1 – 1.5 µm diameter pores were observed under SEM, and images are shown in Figure 3. Many pores were presented as individual ones in the SZ, but there were a few cases that multiple pores accumulated and formed pore chains. In addition, more pore chains were observed in the SZ close to the top surface (Figure 3(b)) than that in the middle area (Figure 3(a)). Finally, many of these pores were distributed inside grains but not just along GBs. Outside of SZ, pores were also observed in the TMAZ, as shown in Figure 4. - More pores are observed in the TMAZ than those in the SZ, especially at locations close to the SZ/TMAZ boundary (Figure 4(a), 0.15 mm away from the SZ/TMAZ boundary), indicating helium was formed more actively in the region with high temperature and plastic deformation without recrystallization. Other than individual pores, up to ~20 μm long microcracks, likely due to helium bubble accumulation, were observed in the TMAZ close to the SZ/TMAZ boundary (Figure 4(a)). On the other hand, only a couple of short pore chains, consisting of a few pores, were observed in the TMAZ 1.96 mm to the SZ/TMAZ boundary (Figure 4(b)). Considering recrystallization happened in SZ but not in TMAZ during the FSW, many pores in the SZ may also be located at the pre-FSW GBs.

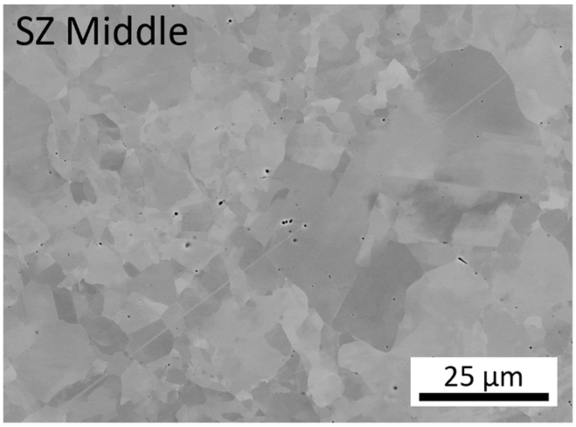

(a) SZ middle

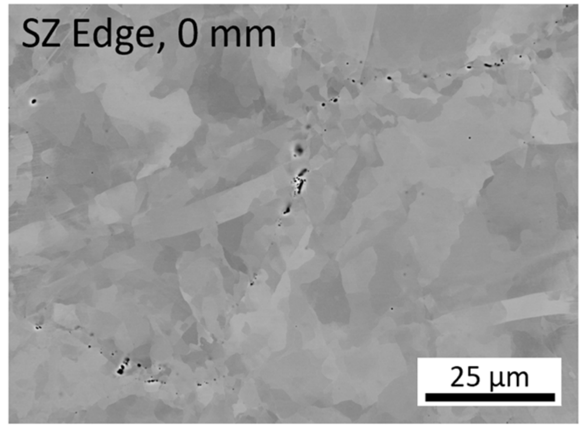

(b) SZ top edge

Figure 3. Pores in the SZ of the irradiated 304L SS friction stir weld.

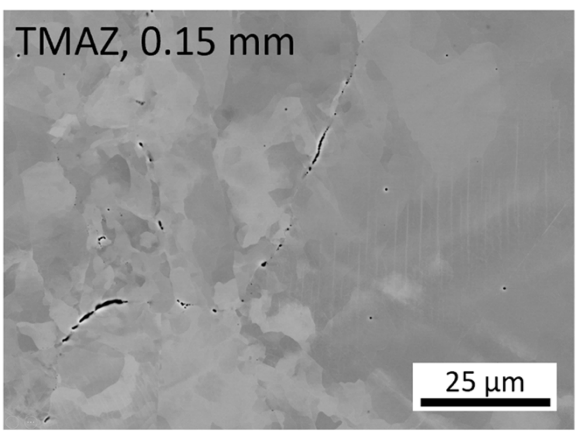

(a) 0.15 mm from the TMAZ/SZ boundary

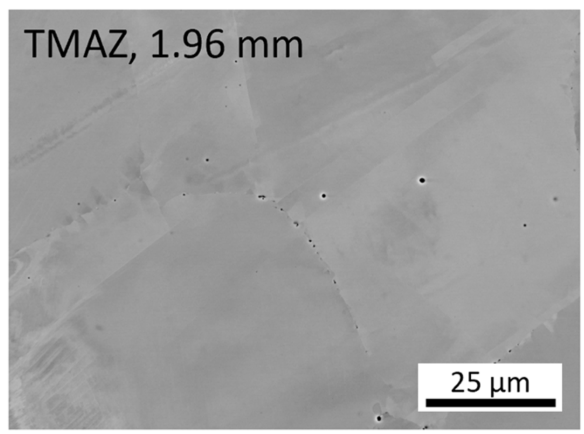

(b) 1.96 mm from the TMAZ/SZ boundary

Figure 4. Pores in the TMAZ of the irradiated 304L SS friction stir weld.

Fine recrystallized grains were observed in the SZ of the 304L SS friction stir weld, similar with conventional material friction stir welds. Grain microstructures in the SZ center, SZ bottom and the BM, taken by SEM/EBSD, are shown in Figure 5. Comparing with grains at the SZ center, grain sizes at the SZ bottom are even tinier because of the low peak temperature during FSW.

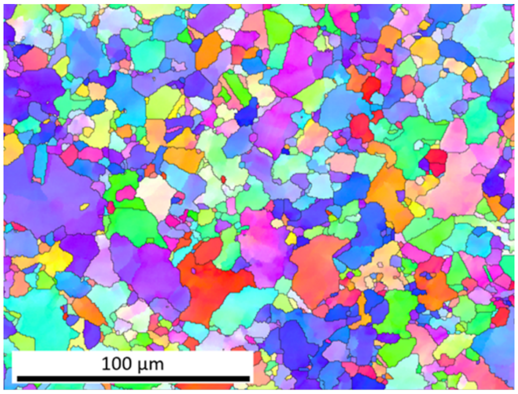

(a) SZ center grains

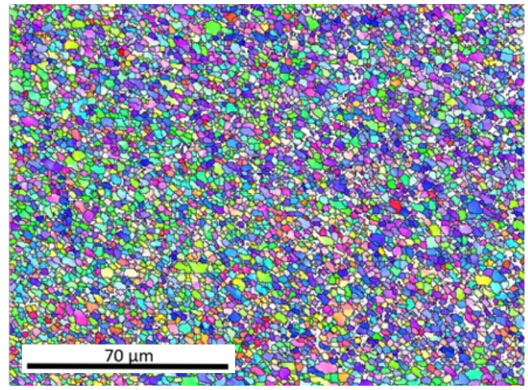

(b) SZ bottom grains

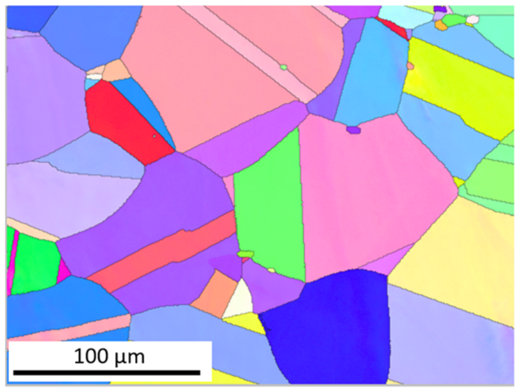

(b) BM grains

Figure 5. IPF images of the SZ center, SZ bottom, and BZ.

Mechanical Properties

Tensile curves of tested specimens are shown in Figure 6. Overall, all specimens were ductile and failed with a large elongation (> 60%). Tensile properties of different specimens containing different metallurgical zones at the gauge areas are shown in Table 2. The BM specimen has the highest yield and ultimate strengths, 386.5 MPa and 595 MPa, respectively. The two TMAZ specimens had relatively low yield strength among all friction stir weld specimens, which were 75% and 81% of the BM specimen yield strength. The TMAZ specimen on the retreating side and the weld root specimen which also contained TMAZ in gauge area had relatively low ultimate strength among all friction stir weld specimens, measured 86% of the BM ultimate strength. Elongations of all friction stir weld specimens are high and those of the SZ specimen and TMAZ specimen on the advancing side are even higher than that of the BM specimen. In conclusion, strengths and elongation of the friction stir weld processed on the irradiated 304L SS are close to the BM, probably contributed by the fine equiaxed grain structures in the SZ and the suppression of helium bubbles formation and accumulation. The weld specimen slightly lower yield strength than that of the BM specimen is probably due to the thermal aging during the FSW.

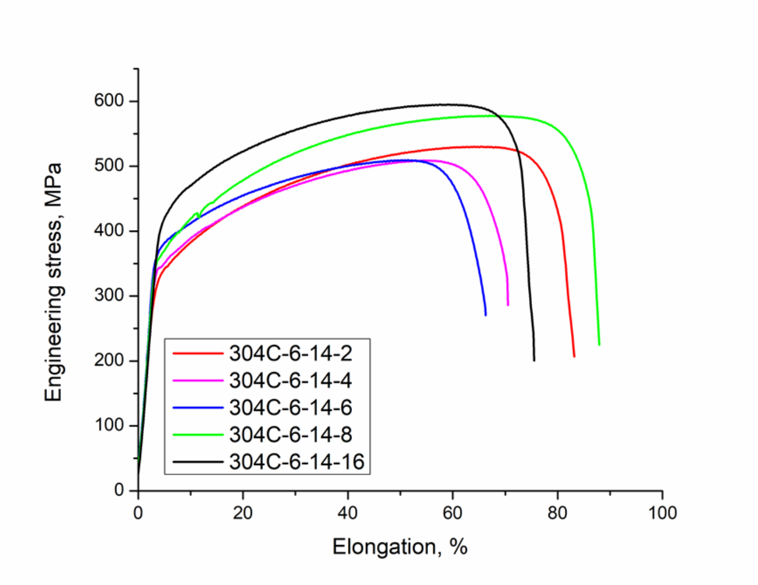

Figure 6. Tensile curves of specimens from different metallurgical zones in the irradiated 304L SS friction stir weld and BM. The gauge length was 2.5 mm.

Table 2. Mechanical properties of the friction stir weld and BM specimens.

Specimen ID	Locations	Yield strength, MPa	Ultimate strength, MPa	Elongation, % (2.5 mm gauge)
304C-6-14-2	¼ depth advancing side	289.0	530.2	81.2
304C-6-14-4	¼ depth retreating side	314.8	509.0	68.0
304C-6-14-6	Weld root	344.5	509.5	64.0
304C-6-14-8	¼ depth SZ middle	338.7	578.1	85.6
304C-6-14-16	BM	386.5	595.0	73.1

CONCLUSIONS

1. The irradiated 304L SS friction stir weld cross-section specimen showed no macro helium induced cracking, which was always seen in irradiated steel fusion welds containing a similar amount of helium. FSW could be a potential technique for irradiated nuclear reactor structural materials repair welding.
2. 1 – 1.5 µm size pores, likely helium bubbles, were observed in the SZ and TMAZ of the friction stir weld cross-section specimen. Pores may be accumulated together to form pore chains and up to ~20 µm microcracks in the TMAZ, and the most severe microcracks were observed in the TMAZ close to the SZ/TMAZ boundary because of the high peak temperature and plastic deformation without recrystallization.
3. All miniature tensile specimens obtained from different metallurgical zones showed ductile behavior with high strengths in tensile tests. The minimum weld specimen yield strength, tensile strength, and elongation were 75%, 86%, and 88% of those of the BM specimen, respectively. Pores and microcracks in the SZ and TMAZ didn't dramatically affect weld specimen's room temperature? mechanical properties.

ACKNOWLEDGEMENTS

The authors gratefully acknowledge ORNL facilities, people, and teams who worked on irradiated material, coupon, and specimen preparation, transportation, handling, and preparation: ORNL's REDC, IMET, and LAMDA facilities, and ORNL's Material's Joining group. We would like to thank personally A. Smith, K. Kinney, C. S. White, C. Crawford, M. Delph, C. Morris, T. Davis, R. Bowman, S. Thurman, K. Smith, B. Sitterson, J. Schmidlin, X. Hu, L. Hulsey, P. Tedder, T. Dixon, M. Mcalister, Z. Feng, J. Chen, R. Miller, S. Clark, K. Leonard, A. Frederick, and D, Kyle at ORNL and G. Frederick, J. Tatman, B. Sutton at the Electric Power Research Institute. The authors appreciate Y. Wang and W. Zhong for their technical reviewing of this paper.

This project is funded jointly by the U.S. Department of Energy, Office of Nuclear Energy, Light Water Reactor Sustainability Program, the Electric Power Research Institute, Long Term Operations Program, and the Welding and Repair Technology Center, with additional support from Oak Ridge National Laboratory.

REFERENCES

1. W. R. Kanne, Jr., "Remote Reactor Repair: GTA Weld Cracking Caused by Entrapped Helium." Welding Journal 67, 8 (1988): pp. 33 – 39.
2. K. Asano, S. Nishimura, Y. Saito, H. Sakamoto, Y. Yamada, T. Kato, T. Hashimoto, "Weldability of Neutron Irradiated Austenitic Stainless Steels," Journal of Nuclear Materials 264, (1999): pp. 1 – 9.
3. M. M. Hall, Jr. A. G. Hins, J. R. Summers, and D. E. Walker, "Weldements: Physical Metallurgy and Failure Phenomena," Proceeding 5th Bolton Landing Conference, (Schenectady, NY: 1978).
4. H.T. Lin, M.L. Grossbeck, and B.A. Chin, "Cavity Microstructure and Kinetics during Gas Tungsten Arc Welding of Helium-Containing Stainless Steel," Metallurgical Transactions A, 21A (1990): 2585 – 2596.
5. S.H. Goods and N.Y.C. Yang, "Microstructural Damage and Residual Mechanical Properties in Helium-Bearing Gas Metal Arc Weldments," Metallurgical Transactions A, 23A (1992): 1021 – 1032.
6. C.A. Wang, M.L. Grossbeck, B.A. Chin, "Threshold Helium Concentration Required to Initiate Cracking During Welding of Irradiated Stainless Steel," Journal of Nuclear Materials, 225 (1995): 59-68.
7. S. Kawano, F. Kano, C. Kinoshita, A. Hasegawa, K. Abe, "Effect of Weld Thermal Cycle, Stress and Helium Content on Helium Bubble Formation in Stainless Steels," Journal of Nuclear Materials, 307–311 (2002): 327–330.
8. R.S. Mishra, Z. Ma, "Friction stir welding and processing", Mater. Sci. Eng. R Rep. 50 (2005): 1–78.
9. D. Lohwasser, Z. Chen, "Friction stir welding: From basics to applications", Elsevier, 2009.
10. W. Tang, M. Gussev, Z. Feng, B. Gibson, R. Miller, J. Chen, S. Clark, K. Leonard, J. Tatman, B. Sutton, G. Frederick, "Friction Stir Welding and Preliminary Characterization of Irradiated 304 Stainless Steel", ASME 2019 Press. Vessels Pip. Conf., PVP2019-93899, (San Antonio, TX: ASME, 2019).
11. B.T. Gibson, W. Tang, A.G. Peterson, Z. Feng, G.J. Frederick, "Evaluating the potential for remote in-process monitoring of tool wear in friction stir welding of stainless steel", J. Manuf. Sci. Eng. 140 (2018): 021012-1 – 021012-11.
12. W. Tang, J. Chen, B. Gibson, R. Miller, S. Clark, M. Vance, Z. Feng, K. Leonard, J. Tatman, B. Sutton, G. Frederick, "Advanced Welding Technology Development for Nuclear Reactor Repair". 2018 International Congress on Advances in Nuclear Power Plants, (Charlotte, NC: ANS, 2018), p. 67.
13. Z. Feng, R. Miller, J. Chen, W. Tang, S. Clark, B. Gibson, M. Vance, G. Frederick, J. Tatman, B. Sutton, "Complete Report on the Development of Welding Parameters for Irradiated Materials", ORNL/SPR-2017/568 (Oak Ridge National Laboratory, 2017).